EFFECT OF NONCONDUCTING SIDE WALLS ON INDUCED END ELECTRIC CURRENTS

Yu. F. Kashkin

The effect of conditions governing the closing of induced electric currents on the total electrical and dynamical characteristics of the motion of a plasmoid through the rectangular channel of an electric-discharge tube in a nonuniform transverse magnetic field was investigated. It was shown that the electric current can be cut to half by introducing a fairly long and thin nonconducting side wall into the channel in the zone of end currents. The length of the inserted side wall must be not less than 6 channels in order to keep the axial electric current from flowing around the side wall.

An experimental investigation of the motion of a plasmoid through a nonuniform transverse magnetic field in a rectangular channel has been presented elsewhere by the present author [1] and by other authors [2], demonstrating the influence exerted by the magnetic-field nonuniformity in the entry zone of the magnet on the plasma flow velocity. Results of an experimental investigation of end electric currents induced in the magnet entry zone and magnet exit zone and of the intrinsic magnetic fields associated with the end currents themselves can be found in another article by the present author [3]. It has been shown that the magnitude of the end currents and of the magnetic fields is influenced by the anisotropy of the plasma conductivity and by stagnation of the stream, and comparisons with predicted data based on formulas derived in [4] are also published in [3].

The nonconducting side walls have to be inserted in order to cope with end effects [5] in the region of end currents. An analytical investigation of the effect of membranes inserted into the channel of an MHD generator and placed outside the electron zone, assuming side walls of infinite length, can be found in [6], while [7] deals with the case where side-wall lengths are considered finite. It has been shown [7] that insertion of such a side wall is effective if the side-wall length is as great as ten channel sizes. Just what the effect of the closing conditions of the electric current is on the total characteristics and dynamics of the plasmoid remains obscure in [1] and [3].

1. Experimental investigations were performed in the rectangular channel of an electric-discharge tube of cross section 3×4 cm, at a distance on the order of 1 m from the discharge chamber. The externally applied nonuniform magnetic field was established with the aid of coils in the form of a Helmholtz pair enclosing the channel on two sides. Preliminary experimental and theoretical estimates of the plasma characteristics ahead of the entry to the magnetic field, which will be designated by the subscript "plus," yielded the following approximate values of the relevant parameters: concentration of charged particles $n_{e+} \approx 10^{17}$ cm^{-3}, temperature $T_+ \approx 18{,}000$°K, plasma flow velocity $u = 2.8 \cdot 10^6$ cm/sec, Mach number of stream ~ 5, electrical conductivity of plasma $\sigma_+ \approx 100$ mho/cm, and time required for plasma to traverse magnetic field $t \approx 100$ μsec. Argon was the working gas in the experiments and was assumed to be completely ionized under the conditions stated.

The dimensionless ratios calculated on the basis of the values of those variables are the magnetic Reynolds number R_m, the magnetohydrodynamic interaction parameter N, and the Hall parameter β, in accordance with the formulas

---

Moscow. Translated from Zhurnal Prikladnoi Mekhaniki i Tekhnicheskoi Fiziki, No. 6, pp. 116-121, November-December, 1970. Original article submitted May 8, 1970.

$$R_m = \frac{4\pi\sigma_+ u_+ h}{c^2},\ N = \frac{\sigma_+ B_0^2 h}{c^2 \rho_+ u_+},\ \beta = \frac{B_0 \sigma_+}{c e n_{e+}}$$

($B_0 \approx 1$ T, $h = 4$ cm as the channel height).

Here ρ_+ is the plasma density, and e the charge on the electron. We ended up with the values $R_m \approx 14$, $N \approx 2$, $\beta \approx 1$.

2. The effect exerted by the magnetic field on the plasma flow pattern was investigated in a channel of nonconducting material standing 4 cm high. Figure 1 shows the layout of this channel (a – with no side walls, b – with side walls inserted, c – shape of external magnetic field and of pattern of induced end currents in both types of channels). It has been shown [3] that the length of the forward and end loops of the end current in the channel with no side walls was about 2.5 channel sizes (~ 10 cm). The forward loop of current terminates at a distance from the center of the magnet which is slightly shorter than the channel size.

If the length of the nonconducting side wall is less than the length of the loop of end current over the channel axis, then the effect of that length on the end current will be relatively modest. When there is no transverse magnetic field, experiment and calculations both show that placing a side wall 5 channel sizes in length (20 cm) with a sharp leading edge into the channel causes a 5-7% decrease in the plasma flow velocity because of the formation of a shock wave on the leading edge of the plate and because of a growth of the boundary layer over the length of the side wall. The approximate thickness δ_t of the turbulent boundary layer is several millimeters ($\delta_t \approx 0.37 x R_x^{-0.2}$, $x = 20$ cm being the length of the plate) in the case of a completely ionized argon plasma under those conditions, but only a fraction of a millimeter in the case of a laminar boundary layer ($\delta_l \approx 5(\eta x / u_\rho)^{0.5}$), where η is the dynamic viscosity). The experimentally derived boundary-layer thickness determined from measurements of the induced potential difference as well as by means of probes (when measuring voltage-current characteristics) was 0.1 cm at the end of the plate.

When the side wall is more than 2.5 channel sizes long, the shape of the end-current loop undergoes a drastic change; loops of the end current I_2 appear in the top and bottom subchannels (see Fig. 1b), and the end electric current I_3 enveloping the side wall exists up to a certain side-wall length.

A small Rogowski loop was used, as in [3], with an integrating circuit and end-current-loop diameter 0.3 cm in order to measure the end currents. The loop was placed in the top or bottom subchannels (2 in Fig. 1b) so that the part of it lying within the channel would occupy the center of the transverse cross section. The plane of the Rogowski loop was perpendicular to the channel axis and was located at a distance of 1 to 2 channel sizes off the center of the magnetic field B_0. A metallic rod 0.3 cm in diameter was introduced into the subchannel lacking a Rogowski loop in order to keep the unobstructed cross section of the subchannels equal; the rod was inserted in the same plane as the Rogowski loop in the other subchannel (see Fig. 1b, 3).

Figure 2 shows the dependence of the end induced current, in the case of both loops of end current, on the magnitude of the transverse magnetic field in the absence of side walls in the channel (1, 2) and with side walls present in the channel (3, 4). Note that when the side wall is present, the current I_2 measured by the Rogowski loop includes the current I_3 encompassing the side wall. The dependences 1 and 3 refer to the forward loop of end current, while dependences 2 and 4 refer to the rear current loop. The dependence of the end current I_2 of both the forward and rear current loops is the same in form as the dependence of the current I_1 on the magnetic field, in the case of the channel unencumbered by side walls. The electric current I_2 was measured in the channel with the side wall extending 5 channel sizes in length. The side wall was located either at the entrance to the magnetic field, when its trailing edge reached the center of the magnet ($x=0$), or at the exit from the magnet, when its leading edge was located at the center of B_0. Both in the channel with the side wall and in the channel unencumbered by any side wall, the end electric current increases with increasing magnetic field in the forward loop and has a maximum at $B_0 \approx 0.5$ T in the case of the rear current loop.

When a nonconducting side wall extending five channel sizes in length was placed in the channel, the end current in the forward loop fell to 0.47-0.55 of current in the channel with no side wall, and the current in the rear current loop fell to 0.58-0.6 of current in the unencumbered channel, at different magnetic fields. The current I_2 in only one of the subchannels was utilized in order to ascertain the above relationships.

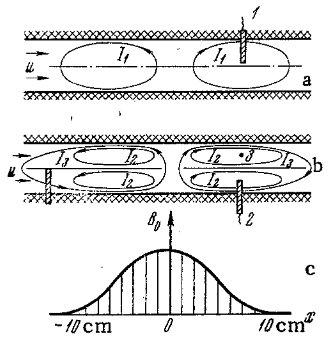

Fig. 1

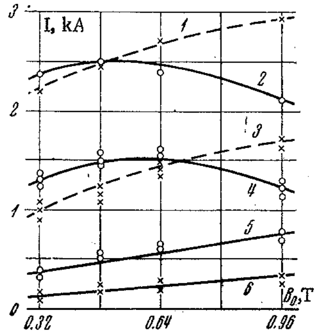

Fig. 2

The electric current was measured with the side-wall length extending from four to six channel sizes in order to determine the effect of the side-wall length on the current I_3 flowing around the side wall. The Rogowski loop was placed in the channel at a distance of three channel sizes from the center of the magnet (Fig. 1b, 1), so that it completely encompassed the top or bottom half of the channel with the side wall separated into two parts.

Figure 2 (5,6) shows the dependences of the electric current on the magnetic field B_0 in the case of side walls extending four and five channel sizes respectively, placed in the zone of the forward current loop. In the case of a side wall extending four channel sizes in length, the current I_3 (5) attained the level of 800 A, and in the case of a side wall extending five channel sizes in length (6), it attained 350 A at $B_0 \approx 1$ tesla. When the side-wall length extended six channel sizes, signals from the Rogowski loop were absent as the magnetic field was increased to 1 tesla, i.e., the current was very small, probably not exceeding 10 A. Hence, when $B_0 \leq 1$ tesla the electric currents flowing around the side wall are practically zero if the length of the side wall is not shorter than six channel sizes. Note that the value of I_3 must be subtracted from the current I_2 in Fig. 2 (3, 4) in order to ascertain the true value of the electric current in the loop above or below the side wall when the latter extends less than six channel sizes in length.

The velocity of the leading edge of the plasmoid was measured at a distance of one channel size beyond the center of the magnet with the aid of two pairs of probes, as was done in [1], in order to obtain an estimate of the influence exerted by the side wall on the flow velocity through changes in the end current and consequently in the braking force. It was found that, when $B_0 \approx 1$ tesla, the velocity of the plasmoid leading edge increases when a side wall extending five channel sizes in length is placed at the entry to the magnet; the increase is from $1.1 \cdot 10^6$ cm/sec to $1.7 \cdot 10^6$ cm/sec and is due to the fall-off of the end current in the forward loop, from 2800 to 1600 A. The extent of the change in velocity does not match the extent of the change in end current. It must be emphasized that the flow velocity was measured in a cross section where the flow velocity through the magnetic field was minimized, i.e., where the leading edge of the plasmoid had already traversed the deceleration zone of the forward and rear current loops. It was pointed out in the experiments that the end electric current in the rear current loop increases and the braking force in the rear current loop increases as the electric current in the forward current loop decreases because of the side wall placed at the entrance to the magnet.

Let us attempt to account for the results on the basis of the simplest theoretical concepts. Using equations describing the distribution of electrical parameters in the channel, we can show [8] that the approximate formula

$$\frac{I}{c^{-1} a\sigma u B_0 h} = C_0 f(R_m, \beta), \qquad C_0 = \text{const} \left(R_m = \frac{4\pi\sigma u h}{c^2}, \ \beta = \frac{B_0 \sigma}{c e n_e} \right) \tag{1}$$

holds when the geometry of the externally applied magnetic field is fixed, with intervals of rapid rise and rapid fall-off in magnetic field coexisting, in the case of channels with no side walls.

Here I is the current in the loop, σ, u, and n_e are the average values of the electrical conductivity, velocity, and concentration of charged particles in the region where the plasma interacts with the magnetic field, and a is the channel dimension in the direction of the magnetic field, whose characteristic value is B_0.

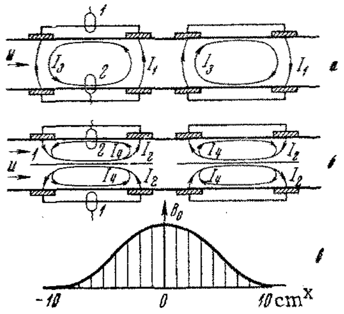

Fig. 3

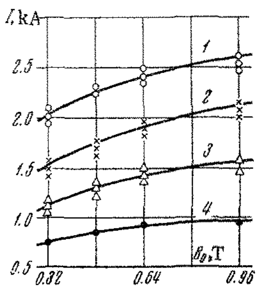

Fig. 4

The function f, representing the dimensionless dissipation of Joule heat in the channel, has been studied in detail by Kholshchevnikova [8].

If we consider the distribution of electrical parameters in a channel of height h/2, with the same geometry of the externally applied magnetic field, the electric current circulating through the loop will be

$$\frac{I}{c^{-1}a\sigma_{0,5}u_{0,5}B_0 l/2h} \approx \frac{C_0}{K} f(R_{m,0.5}, \beta_{0.5}) \tag{2}$$

Here the subscript 0.5 corresponds to the parameters in a channel of height h/2, the function f and the constant C_0 are the same as in Eq. (1), the Reynolds number $R_{m,\,0.5}$ is calculated from the values of $\sigma_{0.5}$, $u_{0.5}$, and h/2, and the Hall parameter is calculated on the basis of the values of $\sigma_{0.5}$ and $n_{e,\,0.5}$. The value of B_0 is the same in either case.

The parameter K takes into account the rate of decline (or of increase) in the specified magnetic field in the channels in question (in relation to the characteristic dimensions h and h/2). In the case where the field declines at a very rapid rate (stepwise varying magnetic field), K is close to unity. When the magnetic field declines more smoothly, $K \approx 1.5$.

Inserting a side wall in the channel all the way to the center of the magnet, where the electric current is practically zero, is equivalent, in a first approximation, to breaking up the channel in the upstream zone of the magnetic field into two subchannels. We therefore have to rely on Eqs. (1) and (2) in order to calculate the currents. The ratio of the current in the loop I in the channel with no side wall to the current in the loop $I_{0.5}$ in the channel with a side wall is expressed by the equation

$$\frac{I}{I_{0.5}} = \frac{\sigma}{\sigma_{0,5}} \frac{u}{u_{0.5}} \frac{2K}{1} \frac{f(R_{m,0.5}, \beta_{0.5})}{f(R_m, \beta)} \tag{3}$$

We estimate the ratio of the variables appearing in the right-hand side of this equation, to begin with. Since the conductivity in the stream of a completely ionized gas does not vary very much over insignificant lengths (and in any case, the variation of the conductivity has much less effect than the variation in velocity), we are safe in assuming

$$\sigma_{0.5} / \sigma \approx 1$$

The ratio of the corresponding Hall parameters and magnetic Reynolds numbers is

$$\frac{\beta_{0.5}}{\beta} = \frac{\sigma_{0.5}}{\sigma} \frac{n_e}{n_{e,0.5}} = \frac{\sigma_{0.5}}{\sigma} \frac{u_{0.5}}{u} \approx \frac{u_{0.5}}{u}$$

$$\frac{R_{m,0.5}}{R_m} = \frac{\sigma_{0.5}}{\sigma} \frac{u_{0.5}}{u} \frac{1}{2} \approx \frac{1}{2} \frac{u_{0.5}}{u}$$

Consider the experimental data for $B_0 \approx 1$ tesla. In that case

$$u_{0.5}/u \approx 3/2, \quad R_{m,0.5}/R_m \approx 3/4, \quad \beta_{0.5}/\beta \approx 3/2$$

Using the data reported in [8], we have

$$f(R_m, \beta) \approx f(3/4 R_m, 3/2 \beta)$$

if $R_m \approx 10$, $\beta \approx 1$. We therefore obtain, from (3), $I_{0.5}/I \approx 0.5$.

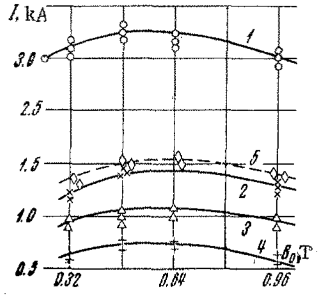

Fig. 5

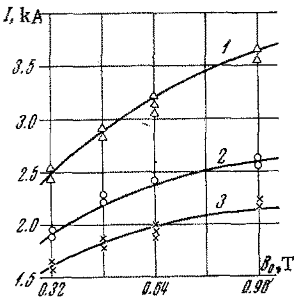

Fig. 6

This corresponds to the experimentally measured current ratio.

The dependence of the current change in the rear current loop in response to increasing B_0 (both in the presence and in the absence of a side wall), plotted in Fig. 2, can be accounted for in terms of the very pronounced total decrease in velocity in the two end current loops.

3. If the top and bottom nonconducting walls of the channel are replaced by continuous copper polished electrodes, in such a way that their boundaries are sufficiently far removed from the boundaries of the external magnetic field, then traces of the overflow of electric current from the plasma into the metal, in the form of cathode spots and anode spots, will remain on the polished surfaces after the experiments have been completed. The top and bottom electrodes were not connected. The ends of the electrodes were placed at $X = \pm 15$ cm ($\sim$4 channel sizes) relative to the center of the magnet, and the boundaries of the magnetic field were placed at $X = \pm 10$ cm (2.5 channel sizes).

Spots were visible on the electrodes moved up to the center of the magnetic field at $-4 < X < 0$ and at $-14 < X < -11$ cm, both on the top and on the bottom magnetic walls. In the zone removed from the center of the magnet ($X < -11$ cm), anode spots showed up on the top electrode, while cathode spots showed up on the bottom electrode. Cathode spots were found on the top electrodes and anode spots were found on the bottom electrode when the electrodes were placed beyond the center of the magnet and in its immediate vicinity ($5 > X > 2$ cm), with the anode situated above and far from the center of the magnet and the cathode situated below ($15 > X > 11$ cm).

The cathode spots near the center of the magnet are much larger and much deeper, on both sides of the magnet, than the spots at some distance from the center of the magnetic field, since $B_0 \approx 1$ tesla at the center of the magnet while $B_0 \approx 0$ at a great distance removed from the center. Consequently, the zones of cathode spots and anode spots on the electrodes coincide with the zones of the boundaries of end-current turns, while the direction of the electric current coincides with the direction indicated in Fig. 1a. The potential differences between probes placed at the center of the magnet, at the same interelectrode spacing and at the same magnitudes of the magnetic field, were compared for the case of a channel with nonconducting walls and a channel with electrodes. The potential difference between the electrodes in the case of a channel with nonconducting walls is much greater than in the case of a channel with electrodes, indicating an increase in the electric current in the zone of entrance to the magnet in the channel with electrodes.

In subsequent experiments, continuous copper electrodes were replaced by nonconducting walls with metallic electrodes 2.5 cm in diameter inserted in them and with the end surfaces of the electrodes lined up flush with the channel walls. The axis of one pair of electrodes, at the magnet entrance, was placed at $X = -3$ cm, the second at $X = -13$ cm. The axis of the first pair of electrodes, at the exit from the magnet, was placed at $X = 3$ cm, the second at $X = 13$ cm. The top electrodes were short-circuited by copper busses, as were the bottom electrodes (see Fig. 3a). The potential difference between the probes at the center of the magnet is the same in the case of the channel with continuous electrodes as in the case of electrodes 2.5 cm in diameter, when the magnitudes of the magnetic field are the same.

Experimental investigation of the end electric currents was performed with the aid of Rogowski loops (1 in Fig. 3a) mounted on the busses connecting the electrodes. The Rogowski loop recorded only the electric current I_1 which entered the electrodes' connecting circuit from the plasma. The dependence of the electric current flowing through the electrodes' circuit is plotted in Fig. 4 (curve 1) and Fig. 5 (curve 1), respectively, for the portion of the channel at the entrance to the magnetic field and for the portion of the channel at the exit from the magnetic field. When the magnetic field was stepped up to $B_0 \approx 1$ tesla, the electric current I_1 (Fig. 3a) flowing through the electrodes increased to 2600 A at the entrance to the magnet and increased to 3000 A at the exit from the magnet.

Measurement of the electric current in the external circuit of the electrodes I_2 in the channel with the nonconducting side walls extending five channel sizes in length and placed in the zone of the entrance to or exit from the magnetic field (Fig. 3b) showed that, at the magnetic-field entrance and exit, the current I_2

flowing through the plasma and through the electrodes (curve 2 in Fig. 4 and in Fig. 5) is less than the current I_1 in the case where side walls are lacking. The current I_2 is at the level of 0.75 to 0.80 of the current I_1 at the entrance to the magnetic field and 0.4 to 0.45 of the current I_1 at the exit from the field.

When the electrodes were introduced into the channel, the loops of end electric current within the channel did not vanish completely, because of the contact resistance present in the electrode sheath (voltage drops at the electrode) (Fig. 3a). Aside from the electric current I_1 flowing through the plasma and through the electrodes, there exists in addition an electric current I_3 flowing within the channel, both at the entrance to and at the exit from the magnet.

The electric currents were measured simultaneously with two Rogowski loops, one to measure the electric current on the bus I_1 and the other inserted in the channel and encompassing half the channel transverse cross section, measuring the current I_3 in the loop within the channel. The electric current I_3 appears before the current I_1, since electric current can appear in the electrodes' circuit only when the leading edge of the plasmoid has traversed the interval separating the pairs of electrodes. If the electric current within the channel increases to a maximum in 4-5 μsec, then the current flowing through the external circuit of the electrodes rises to its maximum in 15 μsec. This time difference can probably be accounted for by the processes involved in forming the electrode spots. When the electric current I_1 attains a maximum, the current within the channel drops to 0.7-0.8 of its maximum value. The maximum values of the electric currents are indicated in Figs. 4 and 5.

The magnetic-field dependence of the end electric current I_3 within the channel with electrodes is plotted in Fig. 4 (curve 3) and in Fig. 5 (curve 3) for the entrance to and exit from the magnetic field, respectively. The end current within the channel I_3 amounts to 0.55-0.62 of current I_1 flowing through the electrodes at the entrance to the magnet and 0.3-0.33 of current flowing at the exit from the magnet, for the maximum values of the electric current.

When nonconducting side walls are placed in a channel with electrodes, end electric currents I_4 within the subchannels (half-channels) are retained (Fig. 3b), even though they are not as large as in a channel with nonconducting walls. Values of the end currents within the subchannels (half-channels) I_4 are plotted in Fig. 4 (curve 4) and Fig. 5 (curve 4) for different magnetic fields. The electric current I_4 is 0.43-0.48 of the value of the current I_2 flowing through the electrodes' circuit in a channel with a plate, at the entrance to the magnet, and 0.4 of that value at the exit from the magnet. The electrical current I_4 within the channel with the electrodes and baffle is 0.55 to 0.58 for the forward turn of the end current and 0.6 to 0.65 for the last turn of the end current, in terms of the fraction of the end current I_3 in the channel with electrodes but without plates.

Consequently, the ratio of the values of electric currents flowing through the end current loops in a channel with side walls to the end current in a channel with no side walls, both in a channel with nonconducting walls and in a channel with electrodes, amounts to 0.5-0.6 at the entrance to the magnet and 0.6-0.65 at the exit from the magnet.

The electrodes, like the side walls, were placed either only at the entrance to the magnet or only at the exit from the magnet, but not both simultaneously, in all of the experiments described above. The value of the end current flowing through the circuit of electrodes at the exit from the magnet is shown in Fig. 5 (curve 1) for the case where the channel has nonconducting walls at the entrance to the magnet. But if electrodes were to be introduced also at the entrance to the magnet, then the value of the end current flowing through the electrodes' circuit at the exit from the magnet would decline abruptly (curve 5 in Fig. 5). For example, when $B_0 \approx 0.5$ tesla, the end currents differ by more than a factor of 2. When the electrodes were introduced at the entrance to the magnet, the total current at the entrance to the magnet increased from 2700 to 3800 A ($B_0 \approx 0.5$ tesla) but decreased from 3300 A to 1500 A in the electrodes' circuit at the exit from the field. The end currents I_4 within the channel differ to a much smaller extent.

This means that the end currents at the entrance to the magnetic field and at the exit from the magnetic field are interrelated, and an increase in one of the end currents is accompanied by a decrease in the other end current because of the increased braking force.

As in the case of the channel with nonconducting walls, measurements were taken of the velocity of the plasmoid leading edge in a cross section located a distance of one channel size beyond the center of the magnet. In a channel with electrodes but with no side wall, the flow velocity is $8 \cdot 10^5$ cm/sec, but $1.3 \cdot 10^6$ cm/sec in a channel with a side wall, at $B_0 \approx 1$ tesla.

The ratio of flow velocities in the case of a channel without a side wall and in the case of a channel with a side wall is more or less the same as in the case of a channel with nonconducting walls. The end electric current in the channel depends both on the flow velocity, magnetic-field gradient, channel geometry, etc. and on the electrical conductivity of the plasma. Measurements taken with electrodes showed that the electrical conductivity of the plasma decreases from 130 to 60 mhos/cm at a distance of 50 cm channel length ($\approx$12.5 channel sizes). The initial interval over which the measurements were taken was located at a distance of 70 cm from the plasma source. The end current in the electrodes' circuit in the zone of the forward current loop varies, at $B_0 \approx 1$ tesla, from 3700 A to 2600 A as the magnet is moved 12.5 channel sizes downstream (Fig. 6).

If the end current increases by a factor of 1.5 with increasing magnetic field from 0.32 tesla to 0.96 tesla at a distance of 70 cm from the plasma source (1 in Fig. 6), then it will increase by only a factor of 1.3 at a distance of 95 cm (2 in Fig. 6) and 120 cm (3 in Fig. 6) from the discharge chamber. The closer the distance to the plasma source, the less the magnetic field will affect the plasma electrical conductivity because of the difference in the variation of the end current in response to increasing magnetic field in different portions of the channel.

The author is indebted to A. B. Vatazhin for kind assistance rendered in the work and for helpful discussions of the article.

LITERATURE CITED

1. Yu. F. Kashkin, "Deceleration of a plasmoid in a nonuniform magnetic field," Zh. Prikl. Mekhan. i Tekh. Fiz., No. 3 (1969).
2. I. I. Demidenko, N. S. Lomino, V. G. Padalka, B. N. Rutkevich, and K. D. Sinel'nikov, "Plasma stream in a nonuniform transverse magnetic field," Zh. Tekhn. Fiz., 39, No. 1 (1969).
3. Yu. F. Kashkin, "Investigation of end electric currents in flow of plasma down the channel of an electric-discharge tube through a nonuniform magnetic field," Zh. Prikl. Mekhan. i Tekh. Fiz., No. 1 (1970).
4. A. B. Vatazhin, "Deformation of velocity profile in a nonuniform magnetic field," Zh. Prikl. Mekhan. i Tekh. Fiz., 31, No. 1 (1967).
5. J. Shercliff, Theory of Electromagnetic Flow Measurement, Cambridge Univ. Press (1963).
6. A. B. Vatazhin and N. G. Nemkova, "Some two-dimensional problems concerning the distribution of electric current in the channel of a magnetohydrodynamic generator with nonconducting side walls," Zh. Prikl. Mekhan. i Tekh. Fiz., No. 2 (1964).
7. I. V. Lavrent'ev, "Effect of length of nonconducting side wall on characteristics of MHD generator," Magnitn. Gidrodinam., No. 1 (1968).
8. E. K. Kholshchevnikova, "Stationary supersonic flow of a conducting gas through a channel with nonconducting walls in the presence of weak magnetohydrodynamic interaction," Zh. Prikl. Mekhan. i Tekh. Fiz., No. 4 (1970).